

Characterization of $\text{Cd}_{1-x}\text{Fe}_x\text{S}$ diluted magnetic semiconductors grown at near phase conversion temperature

X.J. Wu^{a,b}, D.Z. Shen^a, Z.Z. Zhang^a, K.W. Liu^{a,b}, B.H. Li^a, J.Y. Zhang^{a,*}, Y.M. Lu^a, D.X. Zhao^a,
B. Yao^a, X.G. Ren^a, X.W. Fan^a

^a Key Laboratory of Excited State Processes, Changchun Institute of Optics, Fine Mechanics and Physics, Chinese Academy of Sciences, 16 Dongnanhu Road, Changchun 130033, People's Republic of China

^b Graduate School of the Chinese Academy of Sciences, Beijing, 100049, People's Republic of China

Received 25 March 2006; received in revised form 24 October 2006; accepted 7 November 2006 by E.G. Wang
Available online 20 November 2006

Abstract

Fe-based cadmium sulfide alloy thin films have been grown on *c*-plane sapphire substrates by a low-pressure metalorganic chemical vapor deposition technique at different growth temperatures. From X-ray diffraction and absorption spectra of the samples, the evolutions with growth temperature show an inflexion at the growth temperature of 300 °C. This was attributed to the phase transformation from zinc-blende to wurtzite. With increasing growth temperature from 270 °C to 360 °C, Fe concentration in the films increases monotonously. The electronic states of $\text{Cd}_{1-x}\text{Fe}_x\text{S}$ were investigated by X-ray photoelectron spectroscopy. Magnetic measurement shows Van Vleck paramagnetism of the $\text{Cd}_{1-x}\text{Fe}_x\text{S}$ thin film in the temperature region below 7 K.

© 2006 Elsevier Ltd. All rights reserved.

PACS: 60.10.Nz; 68.18.Jk; 73.61.Ga; 78.40.-q; 79.60.-i

Keywords: A. $\text{Cd}_{1-x}\text{Fe}_x\text{S}$; D. Phase conversion; D. Van Vleck-type paramagnetism

1. Introduction

Diluted magnetic semiconductors (DMS) are materials based on II–VI, IV–VI or III–V semiconductors in which a fraction of non-magnetic cations is substituted by magnetic ions like Mn, Fe, Co or rare earths. DMS have recently attracted a great deal of attention, for their possibility of combining ferromagnetic and semiconductor properties in a single material. In the DMS family, Mn based semiconductors have been studied widely. The Mn^{2+} ion possesses only spin momentum ($s = 5/2$, $L = 0$). However, Fe^{2+} possesses both spin and orbital moment ($s = 2$, $L = 2$). Therefore, materials based on Fe are not a simple extension of Mn type DMS. In recent years, many important physical properties of Fe-based II–VI semiconductor materials were studied in theory and experiment, such as $\text{Cd}_{1-x}\text{Fe}_x\text{Te}$, $\text{Cd}_{1-x}\text{Fe}_x\text{Se}$, $\text{Zn}_{1-x}\text{Fe}_x\text{Se}$,

$\text{Zn}_{1-x}\text{Fe}_x\text{S}$, $\text{Zn}_{1-x}\text{Fe}_x\text{O}$ and $\text{Hg}_{1-x}\text{Fe}_x\text{Te}$ [1–5]. However, there are few reports on $\text{Cd}_{1-x}\text{Fe}_x\text{S}$, as far as we know [6–8]. Undoped CdS film is a good material for optoelectronics, piezoelectric transducers and window layers in heterojunction solar cells, etc. [9–11]. Incorporation of Fe ions is expected to bring some novel properties related to spintronics while keeping the outstanding properties of CdS.

In the present paper, well-oriented $\text{Cd}_{1-x}\text{Fe}_x\text{S}$ thin films on *c*-plane sapphire substrates were prepared by low-pressure metalorganic chemical vapor deposition (LP-MOCVD) at different growth temperatures near the phase conversion point. Effects of growth temperature on the structure of $\text{Cd}_{1-x}\text{Fe}_x\text{S}$ films were discussed in detail.

2. Experiment

$\text{Cd}_{1-x}\text{Fe}_x\text{S}$ thin films were grown on *c*-plane sapphire substrates by LP-MOCVD at 270–360 °C, with chamber pressure fixed at about 10 000 Pa by a pressure controller. Before being put into the growth chamber, the sapphire

* Corresponding author.

E-mail address: wuxiaojie555@yahoo.com.cn (X.J. Wu).

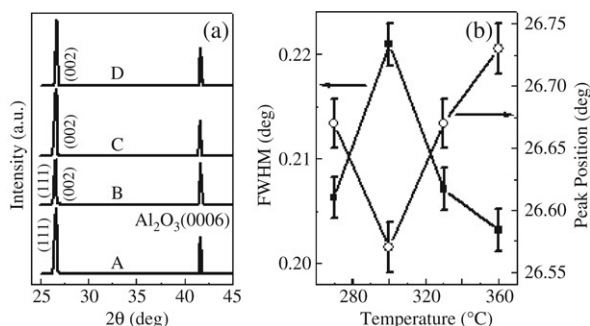


Fig. 1. (a). X-ray diffraction spectra of the $\text{Cd}_{1-x}\text{Fe}_x\text{S}$ thin films deposited on *c*-plane sapphire substrates. The samples grown at 270, 300, 330 and 360 °C were labeled as samples A, B, C and D, respectively. (b) Variations of the FWHM and peak position of the XRD peak with increasing growth temperature.

substrates were firstly cleaned by ultrasonic bathing with a sequence of acetone and ethanol for 5 min, respectively, then chemically polished in $\text{H}_2\text{SO}_4:\text{H}_3\text{PO}_4 = 3:1$ at 160 °C for 10 min and boiled in hydrochloric acid. Dimethyl cadmium (DMCd), iron pentacarbonyl ($\text{Fe}(\text{CO})_5$) and H_2S were used as precursors, flow rates of which were fixed at 3.51×10^{-6} , 3.77×10^{-7} and 1.62×10^{-5} mol/min by separate mass-flow controllers, respectively. High purity hydrogen (99.999%) was used as carrier gas with total flow rate of 1.9 l/min. To minimize pre-reaction, the precursors were separated until approaching to the substrate. Before the growth, the sapphire substrates were annealed at 600 °C in high pure hydrogen ambient for 10 min to remove the residual surface contaminants. The growth was performed for 30 min, and the thickness of samples ranges from 500 to 700 nm, which is measured by the cross section images of the samples on a scanning electron microscope (SEM). The samples grown at 270, 300, 330 and 360 °C were labeled as A, B, C and D, respectively.

The structure of the $\text{Cd}_{1-x}\text{Fe}_x\text{S}$ thin films was characterized by using a rotating anode X-ray diffractometer (Rigaku) with $\text{Cu K}\alpha$ radiation of 0.154 nm. Fe contents were measured by energy dispersive spectroscopy (EDS), and the electronic states of Fe cations were investigated by X-ray photoelectron spectroscopy (XPS). A superconducting quantum interference device (SQUID) was employed to study the magnetic properties of the samples.

3. Results and discussion

Fig. 1(a) shows the X-ray diffraction (XRD) of the $\text{Cd}_{1-x}\text{Fe}_x\text{S}$ thin films prepared at different growth temperatures. Besides the peak at 41.68° from the sapphire, only one diffraction peak located at about 26.7° is observed, which comes from the samples. Fig. 1(b) shows the evolutions of the peak position and the full width at half maximum (FWHM) with increasing the growth temperature. It is obviously that the peak position and the FWHM both show certain changes. Because the Fe doping affects the structure of the films, the electronic states of the doped Fe ions are considered as important factors for these evolutions of the XRD peak.

To determine the electronic states of Fe ions in the $\text{Cd}_{1-x}\text{Fe}_x\text{S}$ thin film, XPS measurements were performed.

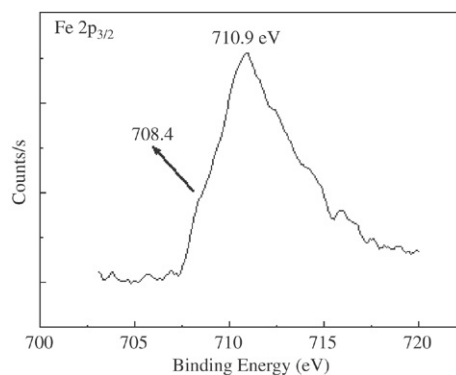


Fig. 2. Fe 2p line of a typical XPS of the samples.

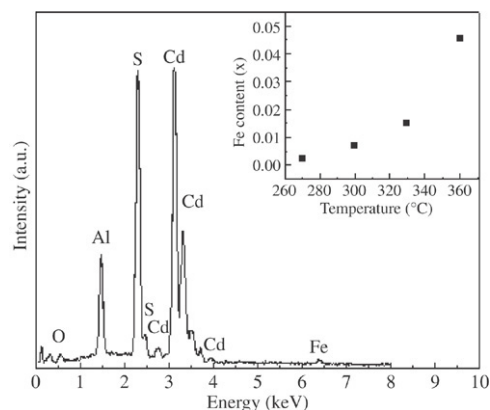


Fig. 3. A typical energy dispersive spectrum (EDS) of the samples. The illustration shows the variation of Fe content in the films with increasing growth temperature.

Fig. 2 shows a typical XPS of the samples. As seen, Fe 2p signals exist as an envelope containing peaks of Fe^{2+} and Fe^{3+} . The shoulder at 708.4 eV is attributed to the contribution of high-spin Fe^{2+} , implying that Fe atoms have been bonded with S atoms in the lattice by replacing some Cd atoms. The peak at 710.9 eV was attributed to the contribution of Fe^{3+} [12]. These triple Fe ions are mainly from the sample surface, which were formed by the oxidation of Fe^{2+} near the surface, because molecular oxygen in air would be absorbed chemically on the exposed sample surface. The oxygen contamination only occurs on the surface, so it would not bring observable effects on the optical absorption of the samples. The effects on the luminescence and electrical properties will be studied elsewhere. In Fig. 2, no signal from Fe^0 was observed, implying there are no iron clusters in the samples.

To ascertain the Fe content in the films grown at different temperatures, energy dispersive spectra (EDS) of the samples were measured. A typical spectrum is shown in Fig. 3. Except for peaks of aluminum and oxygen from the sapphire substrates, Cd, Fe and S peaks come from the $\text{Cd}_{1-x}\text{Fe}_x\text{S}$ thin film. As can be seen distinctly, there is no signal from impurities. Quantitative measurement indicates all the samples are a little cadmium-rich. The illustration in Fig. 3 shows the variation of Fe content in the films with growth temperature. As temperature varies in the range 270–360 °C while keeping precursor flow rates constant, the Fe content shows a monotone increase. This

results from the fact that the high temperature accelerates the pyrolyzing of Fe (CO)₅, which enables more Fe atoms to enter the lattice. Fe contents in samples A, B, C and D are 0.003, 0.007, 0.015 and 0.046, respectively.

Because the radius of the Fe ion (0.076 nm) is smaller than that of Cd²⁺ (0.094 nm), substitution of Fe in the Cd_{1-x}Fe_xS films will decrease the lattice constant. Therefore, in XRD spectra, a continual large-angle-side-shift of the diffraction peak should be observed as Fe content increases. However, in Fig. 1(b), the XRD peak shows an abnormal shift toward the small-angle side for the sample with 0.007 Fe content grown at 300 °C. As is well known, CdS crystal has two phases, metastable cubic and stable hexagonal structures [13]. The difference between the two structures lies only in the stacking sequence along the *c* axis of the hexagonal phase and the (111) axis of the cubic phase, so the (111) peak of cubic CdS is very close to the (002) peak of the hexagonal one (*d* = 0.33590 nm for cubic CdS and *d* = 0.33599 nm for hexagonal CdS). Some groups have reported that the transformation point of CdS from zinc-blende to wurtzite is about 300 °C [14], which is consistent with the temperature where the XRD peak shifts abnormally in Fig. 1(b). Phase conversion at about 300 °C brings restructuring of the lattice of the thin film. The misarranging of atoms results in a certain increase of lattice constant. Therefore, the XRD peak shifts to the small-angle side at 300 °C, though the Fe content increases compared with that of the sample grown at 270 °C. With further increase of growth temperature, the peak shifts gradually to the large-angle side again with increasing Fe concentration. The full width at half maximum (FWHM) of the XRD peak for the films grown at different temperature is also shown in Fig. 1(b). Similar inflexion is also observed at 300 °C. The FWHM of the diffraction peaks (blende (111) or wurtzite (002)) is 0.206, 0.221, 0.207 and 0.203° for samples A, B, C and D, respectively. By using Scherrer's equation $d = 0.94\lambda / (B \cos \theta_B)$, average grain size can be calculated, where λ , θ_B and *B* are the X-ray wavelength (0.154 nm), Bragg diffraction angle and line width, respectively. The calculated grain sizes are 41.4, 38.6, 41.2 and 42.0 nm, respectively. The decrease of grain size for sample B indicates that atom misarranging during phase conversion worsens the crystallization of the Cd_{1-x}Fe_xS thin film. With further increase of growth temperature, the grains enlarge gradually, which benefits from increased surface atom mobility.

To confirm the phase conversion of the Cd_{1-x}Fe_xS films further, absorption spectra were measured at room temperature. For a material with a direct band gap, such as CdS, the optical bandgap is usually obtained from the function $(\alpha hv)^2 - hv$, where α and *hν* denote absorption coefficient and photon energy, respectively. Fig. 4 shows the variation of $(\alpha hv)^2$ vs. *hν* of the samples. The illustration shows the bandgap (*E_g*) of the samples grown at different temperature, which are 2.417, 2.431, 2.421 and 2.419 eV for samples A, B, C and D, respectively. In our other work [15], we have already found that the *E_g* of Cd_{1-x}Fe_xS decreases with increasing Fe content, where the samples were grown at a constant temperature with varying the Fe(CO)₅ flow rate. However, for sample B in the present work, the *E_g* shows a small increase when the Fe content arises

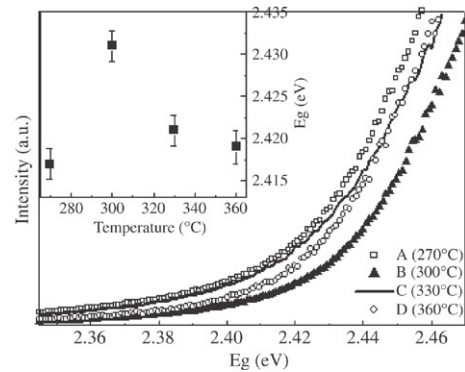


Fig. 4. Variation of $(\alpha hv)^2$ vs. *hν* for samples grown at 270–360 °C. The illustration shows the bandgap *E_g* of the samples grown at different temperature.

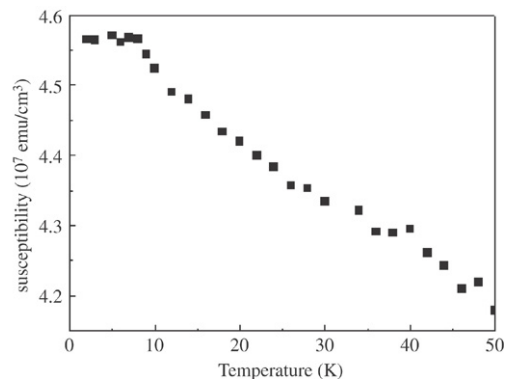


Fig. 5. Temperature dependence of the susceptibility at magnetic field of 500 Oe for sample D.

from 0.003 to 0.007. This is attributed to quantum confinement effects resulting from the smaller grain size of the film, which was obtained at the phase conversion point. For the samples grown beyond 300 °C, the *E_g* decreases monotonically as Fe content rises with increasing growth temperature.

As Fe²⁺ ion is doped into a substitutional site of CdS, the ground state will change into a magnetically inactive single state *A₁* by crystal field and spin–orbit interactions. At low temperature, this state gives rise to a temperature-independent susceptibility, so-called Van Vleck paramagnetism [3,16]. The temperature dependence of the magnetic susceptibility of sample D is shown in Fig. 5, which was measured on a SQUID at fixed magnetic field. As seen, the susceptibility is almost independent of temperature in the range below 7 K. This is a typical characteristic of Van Vleck-type paramagnetism, which was also observed in some reports on other Fe based DMS materials.

4. Conclusions

In conclusion, a series of Cd_{1-x}Fe_xS thin films with different Fe content are prepared by LP-MOCVD at different growth temperature. An abnormal shift of the X-ray diffraction peak was observed at the growth temperature 300 °C and attributed to phase conversion. This conversion affects the evolutions of the X-ray diffraction peak and the optical bandgap of the alloy films. Magnetic susceptibility at low temperature

indicates that the $\text{Cd}_{1-x}\text{Fe}_x\text{S}$ thin film is a Van Vleck-type paramagnetic.

Acknowledgments

This work is supported by the National Natural Science Foundation of China under Grant Nos. 50402016, 60501025 and 60506014, the Key Project of National Natural Science Foundation of China under Grant No 60336020 and No 50532050, the Innovation Project of Chinese Academy of Science.

References

- [1] A. Twardowski, *J. Appl. Phys.* 67 (9) (1990) 5108.
- [2] A. Twardowski, P. Glód, W.J. MdeJonge, M. Demianiuk, *Solid State Commun.* 64 (1987) 63.
- [3] B.T. Jonker, J.J. Krebs, S.B. Qadri, G.A. Prinz, F. Volkening, N.C. Koon, *J. Appl. Phys.* 63 (8) (1988) 3303.
- [4] S.J. Han, J.W. Song, C.H. Yang, S.H. Park, J.H. Park, Y.H. Jeong, *Appl. Phys. Lett.* 81 (2002) 4212.
- [5] A. Twardowski, *J. Appl. Phys.* 73 (1993) 6087.
- [6] A. Twardowski, Y.F. Chen, W.C. Chou, M. Demianiuk, *Solid State Commun.* 90 (1994) 493.
- [7] A. Twardowski, D. Heiman, Y. Shapira, T.Q. Vu, M. Demianiuk, *Solid State Commun.* 82 (1992) 229.
- [8] W.C. Chou, S.S. Kuo, F.R. Chen, A. Twardowski, Y.F. Chen, *Phys. Status Solidi (b)* 193 (1996) 125.
- [9] B. Ullrich, H. Sakai, Y. Segawa, *Thin Solid Films* 385 (2001) 220.
- [10] D.A. Hutchins, J.H. Page, *Appl. Phys. Lett.* 48 (1986) 323.
- [11] Doug H. Rose, Falah S. Hasoon, Ramesh G. Dhere, Dave S. Albin, Rosine M. Ribelin, Xiaonan S. Li, Yoxa Mahathongdy, Tim A. Gessert, Pete Sheldon, *Prog. Photovolt: Res. Appl.* 7 (1999) 331.
- [12] W.M. Skinner, H.W. Nesbitt, A.R. Pratt, *Geochim. Cosmochim. Acta* 68 (2004) 2259.
- [13] C.A. Escoffery, *J. Appl. Phys.* 35 (1964) 2273.
- [14] R. Lozada-Morales, O. Zelaya-Angel, *Thin Solid Films* 281–282 (1996) 386.
- [15] K.W. Liu, J.Y. Zhang, X.J. Wu, B.H. Li, B.S. Li, Y.M. Lu, X.W. Fan, D.Z. Shen, Fe-doped and (Zn, Fe) co-doped CdS films: Could the Zn doping affect the concentration of Fe^{2+} and the optical properties, *Physica B* (in press), Corrected Proof, Available online 4 August 2006.
- [16] N.B. Brandt, V.V. Moshchalkov, *Adv. Phys.* 33 (1984) 193.